Coordination Complexes of Pentamethylcyclopentadienyl Iridium(III) Diiodide with Tin(II) Phthalocyanine and Pentamethylcyclopentadienyl Iridium(II) Halide with Fullerene C 60 – Ani…

ARTICLE *in* ORGANOMETALLICS · MARCH 2015

Impact Factor: 4.13 · DOI: 10.1021/om501210s

9 AUTHORS, INCLUDING:

Dmitri V Konarev
Russian Academy of Sciences
171 PUBLICATIONS **1,929** CITATIONS
SEE PROFILE

Alexey Kuzmin
Institute of Solid State Physics RAS
17 PUBLICATIONS **49** CITATIONS
SEE PROFILE

Salavat Khasanov
Institute of Solid State Physics RAS
303 PUBLICATIONS **2,558** CITATIONS
SEE PROFILE

Rimma Nikolaevna Lyubovskaya
Russian Academy of Sciences
450 PUBLICATIONS **3,723** CITATIONS
SEE PROFILE

ORGANOMETALLICS

Article

pubs.acs.org/Organometallics

Coordination Complexes of Pentamethylcyclopentadienyl Iridium(III) Diiodide with Tin(II) Phthalocyanine and Pentamethylcyclopentadienyl Iridium(II) Halide with Fullerene C_{60}^{-} Anions

Dmitri V. Konarev,*[,†] Sergey I. Troyanov,[‡] Alexey V. Kuzmin,[§] Yoshiaki Nakano,[∥] Salavat S. Khasanov,[§] Akihiro Otsuka,[∥] Hideki Yamochi,[∥] Gunzi Saito,[⊥] and Rimma N. Lyubovskaya[†]

[†]Institute of Problems of Chemical Physics RAS, Chernogolovka, Moscow Region 142432, Russia

[‡]Chemistry Department, Moscow State University, Leninskie Gory, 119991 Moscow, Russia

[§]Institute of Solid State Physics RAS, Chernogolovka, Moscow Region 142432, Russia

[∥]Research Center for Low Temperature and Materials Sciences, Kyoto University, Sakyo-ku, Kyoto 606-8501, Japan

[⊥]Faculty of Agriculture, Meijo University, 1-501 Shiogamaguchi, Tempaku-ku, Nagoya 468-8502, Japan

Supporting Information

ABSTRACT: Synthetic approaches to iridium complexes of metal phthalocyanines (Pc) and fullerene anions have been developed to give three types of complexes. The compound-{$(Cp^*Ir^{III}I_2)Sn^{II}Pc(2-)$}·$2C_6H_4Cl_2$ (**1**) (Cp* is pentamethylcyclopentadienyl) is the first crystalline complex of a metal phthalocyanine in which an iridium(III) atom is bonded to the central tin(II) atom of Pc via a Sn−Ir bond length of 2.58 Å. In $(TBA^+)(C_{60}^{\bullet-})${$(Cp^*Ir^{III}I_2)Sn^{II}Pc(2-)$}·$0.5C_6H_{14}$ (**2**), the {$(Cp^*Ir^{III}I_2)Sn^{II}Pc(2-)$} units cocrystallize with (TBA^+)-$(C_{60}^{\bullet-})$ to form double chains of $C_{60}^{\bullet-}$ anions and closely packed chains of {$(Cp^*Ir^{III}I_2)Sn^{II}Pc(2-)$}. Interactions between the fullerene and phthalocyanine subsystems are realized through $\pi-\pi$ stacking of the Cp* groups of {$(Cp^*Ir^{III}I_2)Sn^{II}Pc(2-)$} and the $C_{60}^{\bullet-}$ pentagons. Furthermore, the spins of the $C_{60}^{\bullet-}$ are strongly antiferromagnetically coupled in the chains with an exchange interaction $J/k_B = -31$ K. Anionic (TBA^+){$(Cp^*Ir^{II}Cl)(\eta^2\text{-}C_{60}^-)$}·$1.34C_6H_4Cl_2$ (**3**) and (TBA^+){$(Cp^*Ir^{II}I)(\eta^2\text{-}C_{60}^-)$}·$1.3C_6H_4Cl_2$·$0.2C_6H_{14}$ (**4**) are the first transition metal complexes containing η^2-bonded C_{60}^- anions, with the $Cp^*Ir^{II}Cl$ and $Cp^*Ir^{II}I$ units η^2-coordinated to the 6−6 bonds of C_{60}^-. Magnetic measurements indicate diamagnetism of the {$(Cp^*Ir^{II}Cl)(\eta^2\text{-}C_{60}^-)$} and {$(Cp^*Ir^{II}I)(\eta^2\text{-}C_{60}^-)$} anions due to the formation of a coordination bond between two initially paramagnetic $Cp^*Ir^{II}Cl$ or $Cp^*Ir^{II}I$ groups and $C_{60}^{\bullet-}$ units. DFT calculations support a diamagnetic singlet ground state of **4**, in which the singlet−triplet energy gap is greater than 0.8 eV. DFT calculations also indicate that the C_{60} molecules are negatively charged.

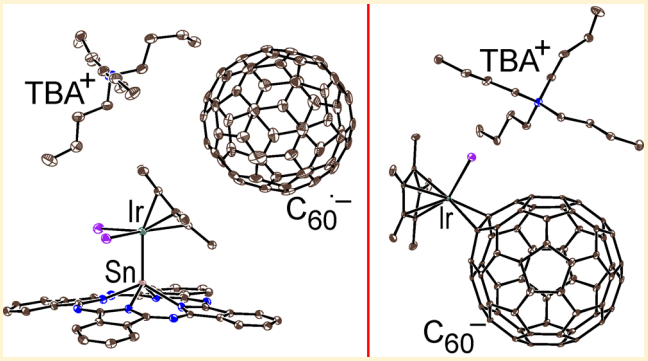

INTRODUCTION

Fullerenes and metal phthalocyanines are widely used in the design of photoactive, magnetic, and conducting compounds.[1] Transition metal complexes of both fullerenes and metal phthalocyanines are of special interest because the coordination of metals can affect their electronic structures and properties. At present, transition metal complexes of fullerenes with palladium, iridium, nickel, cobalt, ruthenium, rhodium, and some other metals are known.[2] The metals are η^2-coordinated to the 6−6 bonds of C_{60} in these complexes. As a result, from one to six metal centers can coordinate to one fullerene molecule,[3] and the metals can link the fullerenes together in the form of dimers or even polymers.[4] Potentially, transition metal complexes of fullerenes with paramagnetic metals can exhibit promising magnetic properties. For example, metal-bridged C_{60} dimers with paramagnetic Co^0 show strong magnetic coupling between spins.[4f] Charge transfer from the metal to the fullerene can provide high conductivity via appropriate packing of fullerene anions in a crystal. However, while low-valent metals generally have strong donor properties, no charge transfer from the metal to fullerene has been detected in transition metal−C_{60} complexes. In fact, these complexes show no absorption bands for C_{60}^- in their NIR spectra, and only a slightly modified IR spectrum for C_{60} is observed.[2d,e,4d−f] One series of anionic transition metal fullerene complexes with metal carbonylates in which the coordination units with fullerene are negatively charged has been reported: (PPN^+)[Co-

Received: December 5, 2014
Published: February 26, 2015

DOI: 10.1021/om501210s
Organometallics 2015, 34, 879−889

Scheme 1

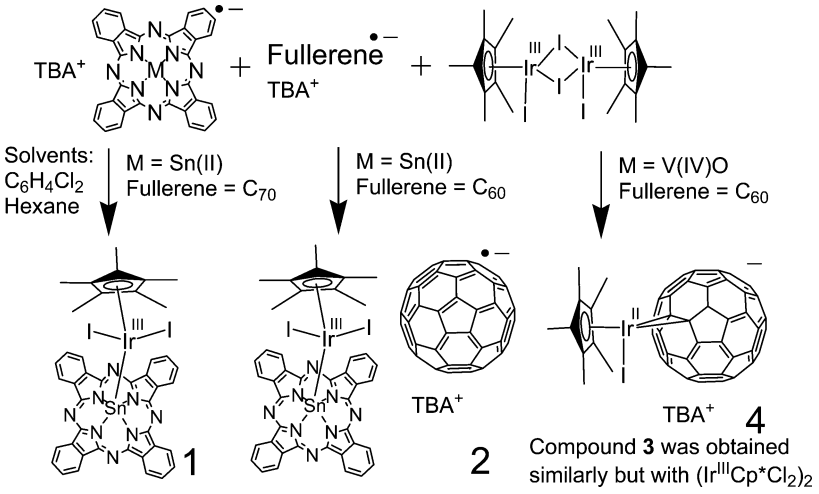

$(CO)_3(\eta^2\text{-}C_{60})]^-$, $(PPN^+)[M(CO)_4(\eta^2\text{-}C_{60})]^-$ (M = Mn and Re), and $(PPN^+)[CpM(CO)_2(\eta^2\text{-}C_{60})]^-$ (M = Mo and W) (PPN^+ is bis(triphenylphosphoranylidene)ammonium cation).[5] The crystal structure of $(PPN^+)[Mn(CO)_4(\eta^2\text{-}C_{60})]^-$ was determined.[5b] Similar anionic complexes with fullerene C_{70} and higher fullerenes have also been prepared.[5c] However, no direct evidence that the C_{60} molecules in these complexes are negatively charged has been uncovered. Absorption bands for C_{60}^- were not observed in the solution NIR spectra of the complexes. Most likely, the negative charge is localized on the transition metal fragment to form anionic carbonylates $[Mn(CO)_4]^-$ or $[CpM(CO)_2]^-$.[5] Consequently, transition metal complexes with fullerene anions remain unknown, and the problem of their synthesis has not yet been solved.

Potentially, metal phthalocyanines and porphyrins can also form coordination complexes with transition metals. Different metal−metal-bonded phthalocyanine and porphyrin dimers are known.[6] Transition metals coordinate via η^6-type bonding to one of the four isoindole subunits of the phthalocyanine (Pc) ligand in substituted metal phthalocyanines. For example, metal octa(ethoxy)phthalocyanine M(PcOEt) (M = H_2, Ni, Cu, VO) reacts with $[Cp^*Ru(MeCN)_3]PF_6$ to form the coordination complex $\{Cp^*Ru[\eta^6\text{-}Ni(PcOEt)]\}PF_6$.[7] In addition, η^5-type complexes of (cymene)Ru^{2+} and Cp^*Ir^{2+} with zinc and nickel octaethylporphyrins were obtained and structurally characterized.[8] Complexes in which manganese, cobalt, and osmium carbonyls and cyclopentadienyl molybdenum tricarbonyl are directly coordinated to the central metal atoms of porphyrins have also been reported for indium, thallium, and tin tetraphenylporphyrins (TPP).[9] With metal phthalocyanine only one coordination compound of such type has been obtained, $Fe(CO)_4(SnPc)$ as a powder,[10] and no crystalline complexes have been reported thus far.

In the present study, new and simple methods for the synthesis of transition metal complexes of metal phthalocyanines and fullerene anions via reaction of their radical anions with the iridium pentamethylcyclopentadienyl dimers $(Cp^*Ir^{III}I_2)_2$ and $(Cp^*Ir^{III}Cl_2)_2$ were developed (Scheme 1). As a result, a crystalline complex of tin(II) phthalocyanine with iridium directly coordinated to the tin atom of the Pc complex was obtained as $\{(Cp^*Ir^{III}I_2)Sn^{II}Pc(2-)\}\cdot 2C_6H_4Cl_2$ (**1**). Although the Sn−Ir bond is well known,[11] this compound is the first crystalline coordination complex of a metal phthalocyanine with this bond. Moreover, the $\{(Cp^*Ir^{III}I_2)Sn^{II}Pc(2-)\}$ units were found to effectively cocrystallize with $(TBA^+)(C_{60}^{\bullet-})$ to form $(TBA^+)(C_{60}^{\bullet-})\{(Cp^*Ir^{III}I_2)Sn^{II}Pc(2-)\}\cdot 0.5C_6H_{14}$ salt (**2**) with closely packed, one-dimensional chains of $C_{60}^{\bullet-}$ and $\{(Cp^*Ir^{III}I_2)Sn^{II}Pc(2-)\}$. Furthermore, $Cp^*Ir^{II}X$ (X = Cl or I, here and throughout the text) fragments also η^2-coordinated to $C_{60}^{\bullet-}$ to form anionic complexes $(TBA^+)\{(Cp^*Ir^{II}Cl)(\eta^2\text{-}C_{60}^-)\}\cdot 1.34C_6H_4Cl_2$ (**3**) and $(TBA^+)\{(Cp^*Ir^{II}I)(\eta^2\text{-}C_{60}^-)\}\cdot 1.3C_6H_4Cl_2\cdot 0.2C_6H_{14}$ (**4**), which are the first transition metal fullerene complexes containing η^2-bonded C_{60}^- anions. All the compounds except **1** are strongly air-sensitive because they contain fullerene anions. The synthesis, crystal structures, and optical and magnetic properties of the four new complexes are discussed.

RESULTS AND DISCUSSION

Synthesis. The reaction steps leading to compounds **1** and **2** are shown in Scheme 1. First, tetrabutylammonium (TBA^+) salts containing tin(II) phthalocyanine and fullerene C_{60} or C_{70} radical anions were generated in the solution according to published procedures.[12,13] The TBA^+ salt of $\{Sn^{II}Pc(3-)\}^{\bullet-}$ can be isolated in crystalline form.[12] Reduction then allowed the dissolution of insoluble $Sn^{II}Pc(2-)$, because the $(TBA^+)\{Sn^{II}Pc(3-)\}^{\bullet-}$ salt was soluble in *o*-dichlorobenzene. The reaction of these salts with $(Cp^*Ir^{III}I_2)_2$ was accompanied by a color change from the deep blue of $\{Sn^{II}Pc(3-)\}^{\bullet-}$ to the green characteristic of neutral tin(II) phthalocyanine. Formation of the coordination complex $\{(Cp^*Ir^{III}I_2)Sn^{II}Pc(2-)\}$ was assumed to be accompanied by oxidation of $\{Sn^{II}Pc(3-)\}^{\bullet-}$. It is likely that electron transfer from $\{Sn^{II}Pc(3-)\}^{\bullet-}$ to $C_{60}^{\bullet-}$ or the reduction of $(Cp^*Ir^{III}I_2)_2$ occurred. No crystalline products were obtained when the pure $(TBA^+)\{Sn^{II}Pc(3-)\}^{\bullet-}$ salt was reacted with $(Cp^*Ir^{III}I_2)_2$. The $(TBA^+)(C_{60}^{\bullet-})$ salt cocrystallized well with $\{(Cp^*Ir^{III}I_2)Sn^{II}Pc(2-)\}$ to form $(TBA^+)(C_{60}^{\bullet-})\{(Cp^*Ir^{III}I_2)Sn^{II}Pc(2-)\}\cdot 0.5C_6H_{14}$ (**2**) in high yield (Scheme 1). In contrast, $(TBA^+)(C_{70}^{\bullet-})$ did not cocrystallize with $\{(Cp^*Ir^{III}I_2)Sn^{II}Pc(2-)\}$, likely due to the larger size of C_{70}. Thus, crystals of individual complex $\{(Cp^*Ir^{III}I_2)Sn^{II}Pc(2-)\}\cdot 2C_6H_4Cl_2$ (**1**) were obtained. It should be noted that $\{(Cp^*Ir^{III}I_2)Sn^{II}Pc(2-)\}$ is stable even in the presence of $C_{60}^{\bullet-}$ and $C_{70}^{\bullet-}$, and no coordination products of $Cp^*Ir^{III}I_2$ to fullerenes were observed under these conditions. A coordination complex of a metal phthalocyanine was therefore synthesized for the first time

DOI: 10.1021/om501210s
Organometallics 2015, 34, 879−889

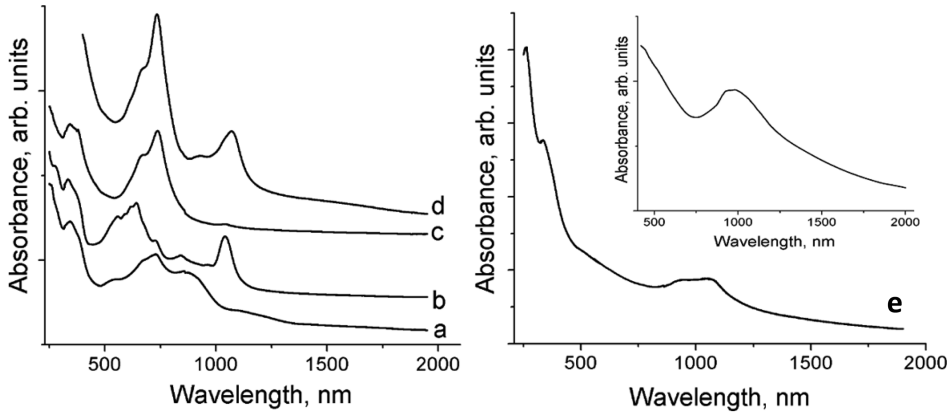

Figure 1. Visible−NIR spectra measured in KBr pellets prepared under anaerobic conditions: (a) neutral $Sn^{II}Pc(2-)$; (b) $(TBA^+)_2\{Sn^{II}Pc(3-)\}^{\bullet-}(Br^-)\cdot$solvent,[12] (c) **1**; (d) **2**; (e) **3**; and (inset) **4**.

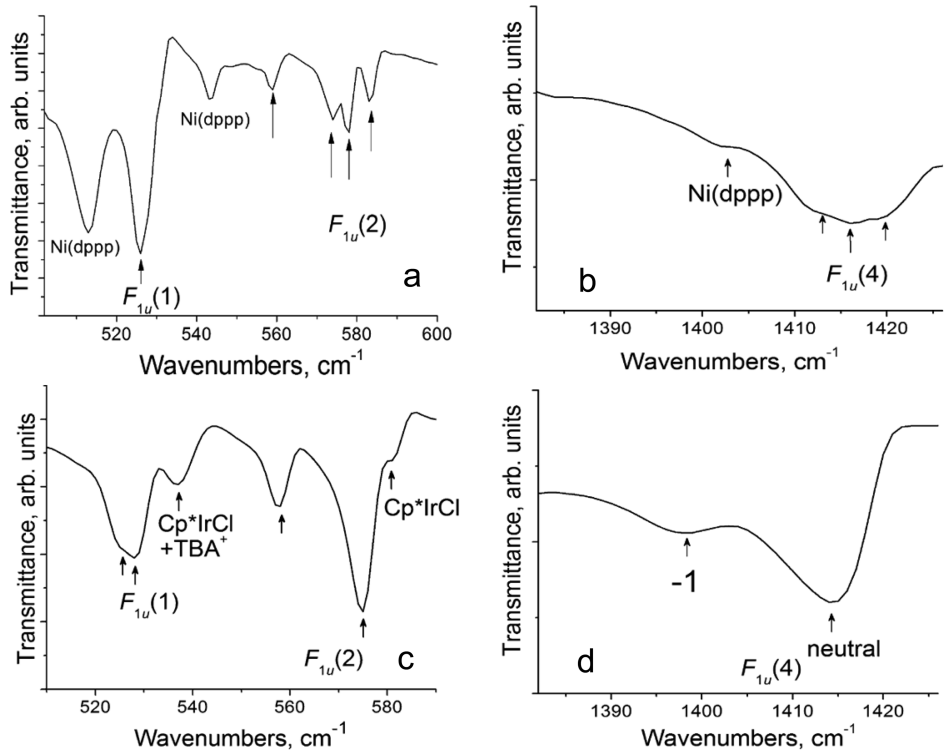

Figure 2. IR-active bands in the spectra of (a) neutral complex$\{Ni^0(dppp)\cdot(\eta^2\text{-}C_{60})\}$ and (c) **3** attributed to the $F_{1u}(1)$ and $F_{1u}(2)$ modes of C_{60} in the 500−600 cm^{-1} range. Absorption bands in the spectra of (b) $\{Ni^0(dppp)\cdot(\eta^2\text{-}C_{60})\}$ and (d) **3** attributed to the $F_{1u}(4)$ C_{60} mode in the 1375−1432 cm^{-1} range.

using radical anions that are highly soluble in organic solvents and reactive toward transition metals. Previously, tetraphenylporphyrin complexes of Sn and In with metal carbonyls have been obtained via the addition of $Hg\{M(CO)_{4-5}\}_2$ (M = Co, Mn) to $Sn^{IV}Cl_2TPP$ or $Co_2(CO)_8$, $Mn_2(CO)_{10}$ to $In^{III}ClTPP$, and osmium carbonyl to indium tetraphenylporphyrin hydride.[9] The compound$\{Fe(CO)_4\}SnPc$ was also obtained via the reaction of $Na_2Fe(CO)_4$ with $Sn^{IV}Cl_2Pc$.[10]

Because the $Cp^*Ir^{III}I_2$ units readily coordinate to $\{Sn^{II}Pc(3-)\}^{\bullet-}$, they cannot be used for the synthesis of pure complexes of $Cp^*Ir^{II}I_2$ with $C_{60}^{\bullet-}$. The radical anion $\{V^{IV}OPc(3-)\}^{\bullet-}$, which has no tendency to form coordination complexes with $Cp^*Ir^{III}I_2$, was therefore used. Reaction of the $(TBA^+)\{V^{IV}OPc(3-)^{\bullet-}\}$ and (TBA^+) $(C_{60}^{\bullet-})$ salts with $(Cp^*Ir^{III}Cl_2)_2$ or $(Cp^*Ir^{III}I_2)_2$ dimers yielded anionic complexes **3** and **4** with the composition $(TBA^+)\{(Cp^*Ir^{II}X)(\eta^2\text{-}C_{60}^-)\}\cdot$solvent, respectively, as crystals. It is clear that the first stage of this reaction was reduction of $Cp^*Ir^{III}X_2$ to $Cp^*Ir^{II}X$ by $\{V^{IV}OPc(3-)\}^{\bullet-}$ (Scheme 1) because insoluble neutral $V^{IV}OPc(2-)$ precipitated from solution. During the second stage, $Cp^*Ir^{II}X$ coordinated to $C_{60}^{\bullet-}$ (Scheme 1). It should also be noted that reaction of the $(TBA^+)(C_{60}^{\bullet-})$ salt with $(Cp^*Ir^{III}I_2)_2$ did not yield any crystalline products.

Spectroscopic Properties. The charged state of tin(II) phthalocyanine and fullerene C_{60} can be estimated from their UV−visible−NIR and IR spectra because the spectra for both the neutral and negatively charged species are known. The formation of the tetrabutyl- and tetraethylammonium salts of $\{Sn^{II}Pc(3-)\}^{\bullet-}$ was accompanied by the appearance of a new intense band in the NIR region at 1040 nm and a blue shift of

DOI: 10.1021/om501210s
Organometallics 2015, 34, 879−889

Table 1. Geometric Parameters for $Sn^{II}Pc(2-)$ and Coordination Units in 1−4

compound	average bond length, Å				displacement of atoms from the 24-atom Pc plane, Å		
	Sn−N(Pc)	Sn−Ir	Ir−I	Ir−C(Cp*)	Sn	$N_{pyrrole}$	$C_{phenyle}$
$Sn^{II}Pc$ (2−)[19]	2.266(3)				1.275	0.107−0.200	0.157−0.617
{($Cp^*Ir^{III}I_2$)$Sn^{II}Pc$} in **1**	2.186(4)	2.5771(3)	2.6846(3)	2.1873(5)	1.144	0.120−0.212	0.378−0.685
{($Cp^*Ir^{III}I_2$)$Sn^{II}Pc$} in **2**	2.188(7)	2.5828(6)	2.6904(8)	2.188(9)	1.136	0.109−0.209	0.185−0.689

	average length of bonds, Å						
	Ir−C(C_{60})	Ir−halogen	Ir−C(Cp*)	coordinated 6−6 bond in C_{60}	adjacent 5−6 bonds	other 6−6 bonds in C_{60}	other 5−6 bonds in C_{60}
($Cp^*Ir^{II}Cl$)(η^2-C_{60}^-) in **3**	2.131(10)	2.433(9)	2.187(11)	1.521(14)	1.488(16)	1.382(16)	1.452(16)
($Cp^*Ir^{II}I$)(η^2-C_{60}^-)} in **4**							
1 unit	2.131(9)	2.6116(8)	2.209(11)	1.529(14)	1.481(14)	1.389(16)	1.452(16)
2 unit	2.123(10)	2.5987(8)	2.200(10)	1.532(13)	1.480(14)	1.396(16)	1.443(16)

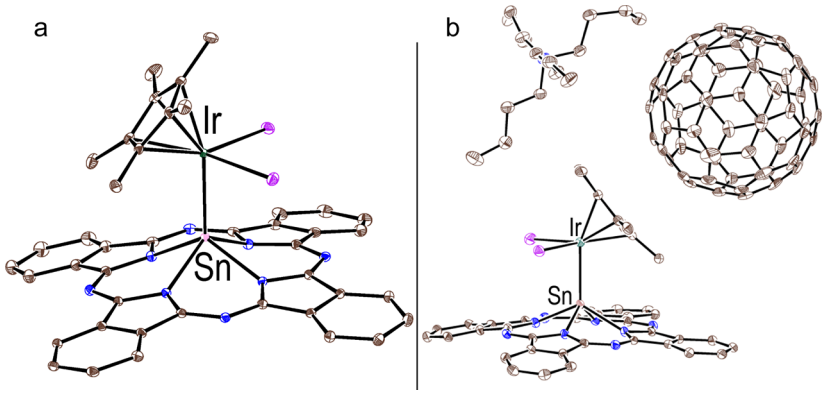

Figure 3. Crystallographically independent units in **1** (a) and **2** (b). Solvent molecules are not shown. Ellipsoid probability is 25%.

the Q-band from 729 nm in the spectrum of $Sn^{II}Pc(2-)$ (Figure 1a) to 642 nm in the spectrum of the $(TBA^+)_2${$Sn^{II}Pc(3-)$}$^{\bullet-}$(Br^-)·solvent salt (Figure 1b).[12] Such changes were previously observed for radical anions of various metal phthalocyanines in which the negative charge was delocalized over the Pc ligand.[12,13] The Q-band in the spectrum of **1** (Figure 1c) is split and positioned at 670 and 734 (maximum) nm. The maximum of the Q-band remains nearly unchanged relative to that in the spectrum of starting $Sn^{II}Pc(2-)$ (729 nm). In addition, no band of {$Sn^{II}Pc(3-)$}$^{\bullet-}$ was observed at 1040 nm (Figure 1c), indicating that no charge transfer to the Pc ligand occurred in **1**. It can therefore be concluded that the $Cp^*Ir^{III}I_2$ group is too weak a donor to reduce the macrocycle in $Sn^{II}Pc(2-)$.

Cocrystallization of {($Cp^*Ir^{III}I_2$)$Sn^{II}Pc(2-)$} with (TBA^+)-($C_{60}^{\bullet-}$) in **2** did not change the charged state of $Sn^{II}Pc$ in comparison to **1** because the positions of the Q-bands in the spectrum of **2** at 668 and 734 (maximum) nm (Figure 1d) are close to those in the spectrum of **1** (Figure 1c). The bands in the spectrum of **2** at 933 and 1066 nm can be attributed to the $C_{60}^{\bullet-}$ radical anions, which generally show these bands at 930−950 and 1060−1080 nm, respectively.[14] The IR spectrum of **2** also indicates the formation of $C_{60}^{\bullet-}$ (Table S1 and Figure S2 in the Supporting Information) because the absorption band for the $F_{1u}(4)$ C_{60} mode is shifted from 1429 cm^{-1} (neutral C_{60}) to 1392 cm^{-1} in the spectrum of **2**. The peak for this mode in the spectra of the $C_{60}^{\bullet-}$ salts appears at 1388−1396 cm^{-1}.[14,15] In addition, the negative charge on C_{60} essentially increases the intensity of the $F_{1u}(2)$ C_{60} mode at 576 cm^{-1} relative to that of the $F_{1u}(1)$ mode at 526 cm^{-1} (Figure S2). Thus, the negative charge in **2** resides on the $C_{60}^{\bullet-}$, and no transfer of electron density from $C_{60}^{\bullet-}$ to {($Cp^*Ir^{III}I_2$)$Sn^{II}Pc(2-)$} occurs in the ground state.

The UV−visible−NIR spectra of **3** and **4** are shown in Figure 1e and the inset in Figure 1, right panel, respectively. Two main bands of C_{60} are observed in the UV range of the spectrum for **3** at 260 and 336 nm. No bands attributed to charge transfer from the metal to C_{60} in the visible range, which are observed for neutral transition metal C_{60} complexes and are responsible for their green color, were detected.[2,4] Compounds **3** and **4** in fact are violet-brown in the solid state and generate violet solutions. The most pronounced features of both spectra are the intense bands in the NIR range at 940 and 1040 nm for **4** and 926 and 990 nm for **3**. The positions of the bands are close to those in the spectra of the $C_{60}^{\bullet-}$ salts at 930−950 and 1060−1080 nm.[14] However, the maxima of these bands are slightly blue-shifted and relatively broadened.

Next, the IR spectrum of **3** was compared to that of {Ni^0(dppp)·(η^2-C_{60})} (dppp is 1,3-bis(diphenylphosphino)-propane) containing neutral C_{60}[2d] (Figure 2). In the IR spectrum of {Ni^0(dppp)·(η^2-C_{60})} the absorption band for the $F_{1u}(1)$ C_{60} mode has essentially stronger intensity than the split band of the $F_{1u}(2)$ mode (Figure 2a) and is characteristic of neutral C_{60}.[15] The $F_{1u}(4)$ mode is split into three bands, at 1412, 1416, and 1419 cm^{-1} (Figure 2b); the slight shift of this band relative to 1429 cm^{-1} is attributed to π-back-donation.[2c−f] Contrary the absorption band for the $F_{1u}(2)$ C_{60} mode in the spectrum of **3** has essentially higher intensity than the $F_{1u}(1)$ C_{60} mode (Figure 2c) and is even characteristic of the $C_{60}^{\bullet-}$ salts[14,15] The absorption band of the $F_{1u}(4)$ mode is located in

DOI: 10.1021/om501210s
Organometallics 2015, 34, 879−889

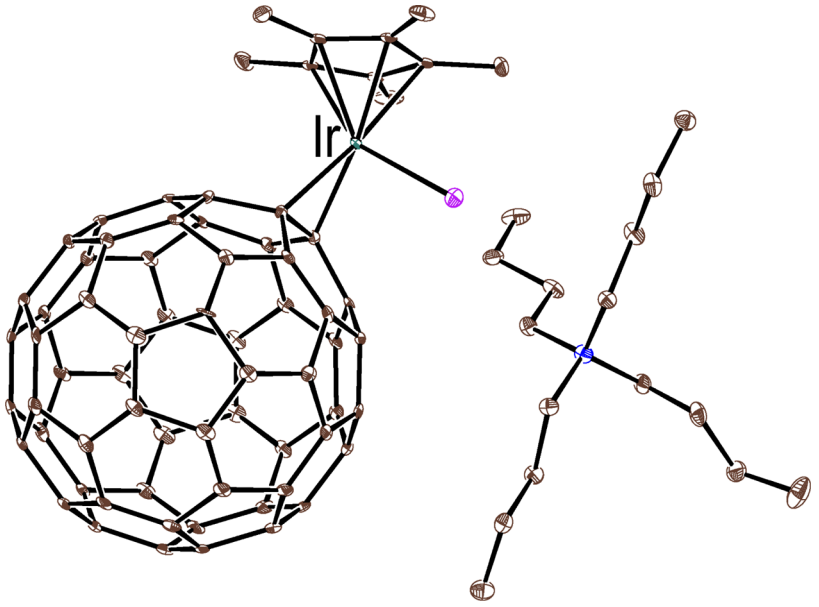

Figure 4. Crystallographically independent units in **4**. Solvent molecules are not shown. Ellipsoid probability is 25%.

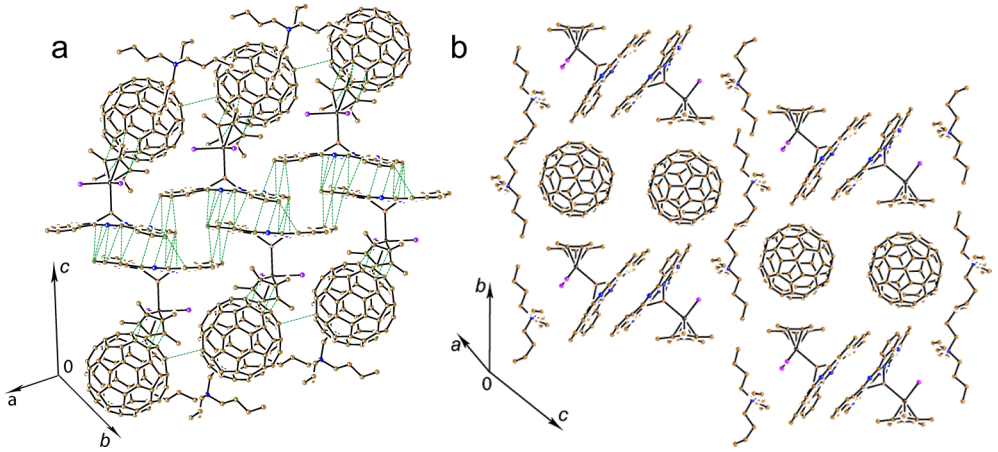

Figure 5. (a) View of the fullerene and phthalocyanine chains in **2**. Short van der Waals C···C and C···N contacts are indicated by green dashed lines. (b) View along the fullerene and phthalocyanine chains.

the spectrum of **3** at 1414 cm^{-1} (Figure 2d); weak red shift of this mode relative to 1429 cm^{-1} can also be explained by π-back-donation.[2c−f] The position of new band of the $F_{1u}(4)$ C_{60} mode in the IR spectrum of **3** at 1398 cm^{-1} (Figure 2d) indicates the presence of the C_{60}^- anions. The IR spectrum of **4** shows similar features (see Supporting Information, Table S1 and Figure S4). Thus, there are obvious differences between the IR spectra of **3** and **4** and neutral complex $\{Ni^0(dppp)\cdot(\eta^2\text{-}C_{60})\}$.

Because the $Cp^*Ir^{II}X$ species coordinate to the $C_{60}^{\bullet-}$ during the synthesis of **3** and **4**, initially an ionic $(TBA^+)\{(Cp^*)^-Ir^{II}(X^-)\}(\eta^2\text{-}C_{60}^-)\}$ complex forms. However, $C_{60}^{\bullet-}$ is a strong reductant with a first oxidation potential of −0.44 V.[16] Therefore, $C_{60}^{\bullet-}$ can potentially reduce $Cp^*Ir^{II}X$ to $Cp^*Ir^{I}X$ and form neutral C_{60} in $(TBA^+)\{(Cp^*)^-Ir^{I}(X^-)\}(\eta^2\text{-}C_{60}^0)\}^-$. However, according to optical data, C_{60}^- anions are present in **3** and **4**. Thus, these anions coexist with $Cp^*Ir^{II}X$. Most likely the Cp* ligands strongly enhance the donor ability of the Ir^{II} atoms, preventing their reduction by C_{60}^-. It has been previously shown that decamethylmetallocenes ($Cp^*_2M^{II}$, M = Ni, Cr, Co) have strong donor properties[17] and can reduce fullerenes to the −1, −2, and even the −3 charge state.[18]

Crystal Structures. Selected bond lengths and atom displacements from the 24-atom Pc plane in the coordination units with tin(II) phthalocyanine and C_{60} are listed in Table 1. The $\{(Cp^*Ir^{III}I_2)Sn^{II}Pc(2-)\}$ species have similar geometries in **1** and **2** (Figure 3a and b), with the $Cp^*Ir^{III}I_2$ units coordinated to the central tin atoms of $Sn^{II}Pc(2-)$ through Sn−Ir bonds, each with a length of 2.58 Å. One Cp* ligand and two iodine anions are also bonded to the iridium atom with lengths for the Ir−C(Cp*) and Ir−I bonds ranging from 2.1873(5) to 2.188(9) Å and 2.6846(3) to 2.6904(8) Å, respectively (Figure 3a and b, Table 1). The average equatorial Sn−N(Pc) bonds are shortened from 2.266(3) Å in $Sn^{II}Pc(2-)$[19] to 2.186(4) and 2.188(7) Å in **1** and **2**, respectively. As a result, the displacement of the tin atoms from the 24-atom Pc plane decreases from 1.275 Å in $Sn^{II}Pc(2-)$[19] to 1.136−1.144 Å in **1** and **2**.

Structures of the anions $\{(Cp^*Ir^{II}Cl)(\eta^2\text{-}C_{60}^-)\}$ and $\{(Cp^*Ir^{II}I)(\eta^2\text{-}C_{60}^-)\}$ have been obtained for the first time in **3** and **4** (Figure 4). Previously, only $(Cp^*Ru)_2(\mu_2\text{-}Cl)_2C_{60}$,

DOI: 10.1021/om501210s
Organometallics 2015, 34, 879−889

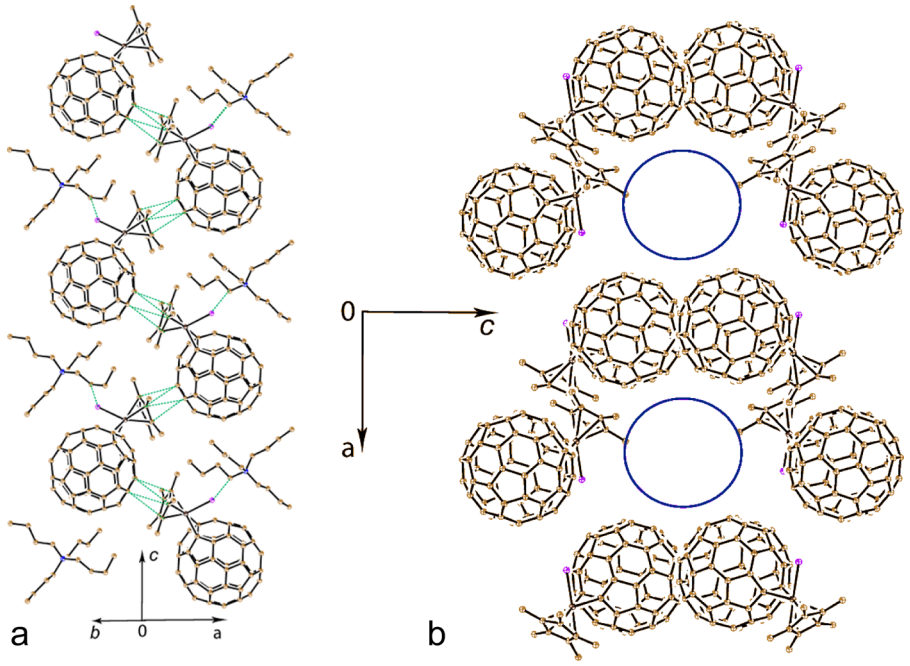

Figure 6. (a) Zigzag chains comprising $\{(Cp^*Ir^{II}I)(\eta^2\text{-}C_{60}^{-})\}$ anions in **4** arranged along the *c*-axis with the TBA^+ cations in the voids; (b) view along the *b*-axis and bulk channels formed by the $\{(Cp^*Ir^{II}I)(\eta^2\text{-}C_{60}^{-})\}$ anions accommodating $C_6H_4Cl_2$ molecules (shown by blue circles).

$(Cp^*Ru)_2(\mu_2\text{-}Cl)(\mu_2\text{-}H)C_{60}$, and $(Cp_2Ti)(\eta^2\text{-}C_{60})\cdot C_6H_5Me$ were reported as structurally characterized fullerene complexes in which a metal atom was coordinated simultaneously to fullerene and cyclopentadienyl or pentamethylcyclopentadienyl ligands.[20] A coordination compound of indenyliridium(I) with C_{60} is also known.[21] The $Cp^*Ir^{II}I$ and $Cp^*Ir^{II}Cl$ fragments are η^2-coordinated to the 6−6 bond of C_{60}. The average $Ir-C(C_{60})$ bond lengths are 2.131(10) Å in **3** and 2.131(9) and 2.123(10) Å in **4** for the two crystallographically independent units. The $Ir-C(C_{60})$ bond lengths in other iridium−C_{60} complexes are reported to range from 2.15 to 2.23 Å.[2b,22] The 6−6 C−C bonds to which the iridium atoms are coordinated in **3** and **4** are elongated to 1.521(14)−1.532(13) Å, while the lengths of the remaining 6−6 bonds in C_{60} range from 1.382(16) to 1.396(16) Å (Table 1). This lengthening effect is attributed to π-back-donation.[2c] Moreover, the coordination of iridium to fullerene results in a slight elongation of the 6−5 C_{60} bonds adjacent to the coordinated 6−6 bond up to 1.480(14)−1.488(16) Å (the average length of other 6−5 bonds in the C_{60} ligands range in length from 1.443(16) to 1.452(16) Å) (Table 1). One Cp* ligand and one chloride or iodine anion are also coordinated to each iridium atom (Figure 4, Table 1).

In complex **1**, the $(Cp^*Ir^{III}I_2)Sn^{II}Pc(2-)$ pairs are arranged in chains via weak C···C contacts (Figure S5). The phthalocyanines are closely packed in pairs with an interplanar distance of 3.391 Å, and six van der Waals C···C contacts are formed within the pairs. However, no $\pi-\pi$ interactions were observed between the pairs due to their mutual orthogonal arrangement (Figure S5).

$(TBA^+)(C_{60}^{\bullet-})\{(Cp^*Ir^{III}I_2)Sn^{II}Pc(2-)\}\cdot 0.5C_6H_{14}$ (**2**) contains closely packed chains of $C_{60}^{\bullet-}$ units running along the *a*-axis (Figure 5). The center-to-center (ctc) interfullerene distance in this direction is 10.15 Å, and one short van der Waals (vdW) C···C contact of 3.22 Å is formed between the fullerenes. Two chains are also arranged quite close to each other because the ctc distance between the $C_{60}^{\bullet-}$ anions in the neighboring chains is only 10.41 Å, although no vdW C···C contacts are formed. Thus, as a whole the packing of $C_{60}^{\bullet-}$ can be considered as double chains that are isolated by the TBA^+ cations (the ctc distances between $C_{60}^{\bullet-}$ in neighboring double chains are even 12.86 Å, Figure 5b). Clearly, the ctc distances between $C_{60}^{\bullet-}$ anions in the chains are sufficiently long to avoid dimerization of $C_{60}^{\bullet-}$ but short enough to manifest magnetic coupling between spins. Each Pc plane of $(Cp^*Ir^{III}I_2)Sn^{II}Pc(2-)$ forms $\pi-\pi$ interactions with three neighboring Pc planes with interplanar distances of 3.368, 3.393, and 3.393 Å. Multiple short vdW C···C and C···N contacts between them result in the formation of the closely packed chains along the *a*-axis (the contacts are indicated by green dashed lines in Figure 5a). The interplay between the fullerene and phthalocyanine subsystems is realized via the $\pi-\pi$ interactions between the Cp* ligands of $\{(Cp^*Ir^{III}I_2)Sn^{II}Pc(2-)\}$ and the $C_{60}^{\bullet-}$ pentagons, which are arranged nearly parallel to each other (the deviation from parallel arrangement is only 3.48°). Five vdW C···C contacts are formed within the 3.25−3.38 Å range. This arrangement suggests that effective charge transfer can be realized in **2** between the fullerene and phthalocyanine subsystems (for example, photoinduced charge transfer).

Packing of the $\{(Cp^*Ir^{II}X)(\eta^2\text{-}C_{60}^{-})\}$ anions in **4**, which is isostructural to **3**, is shown in Figure 6. Zigzag chains of these anions are formed along the *c*-axis, which in turn form vacancies to accommodate the TBA^+ cations (Figure 6a). The anions form weak $\pi-\pi$ interactions via connection through the Cp* ligand located close to the hexagon of the neighboring $\{(Cp^*Ir^{II}X)(\eta^2\text{-}C_{60}^{-})\}$ anion (the vdW C···C contacts fall in the range 2.94−3.67 Å). The angle between the C_{60} hexagon and the Cp* plane is 16−17°, and the fullerene spheres in the $\{(Cp^*Ir^{II}X)(\eta^2\text{-}C_{60}^{-})\}$ anions are isolated. The shortest ctc distance is 10.08 Å, and no vdW contacts are formed between them. On the whole, the structures of **3** and **4** can be described as hexagonal 3D packing with large channels occupied by $C_6H_4Cl_2$ molecules. The channels are arranged along the *b*-axis (indicated by the blue circles in Figure 6b).

DOI: 10.1021/om501210s
Organometallics 2015, 34, 879−889

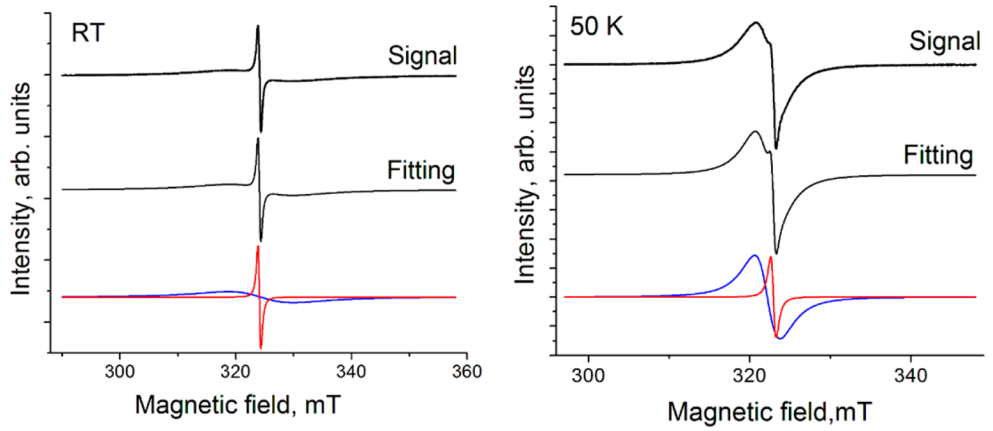

Figure 7. EPR spectra of **2** at RT (294 K) and 50 K. The fitting of the signals using two Lorentzian lines is also shown.

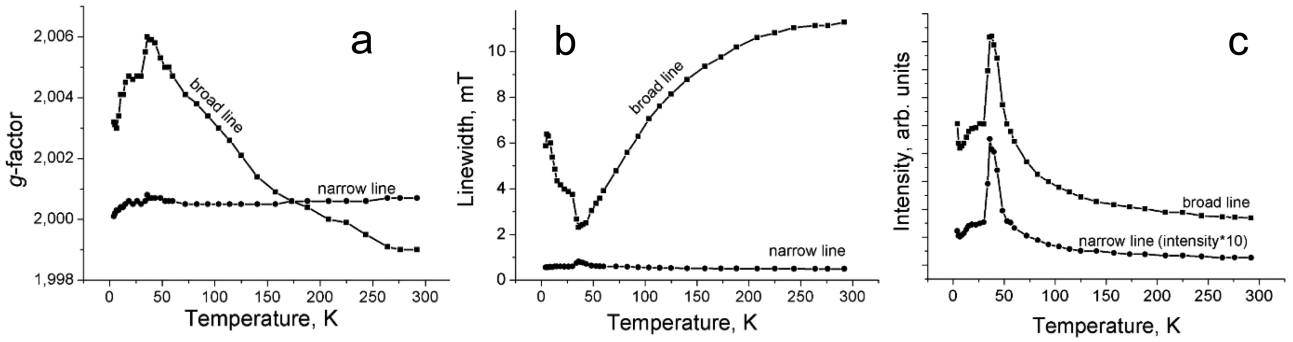

Figure 8. Temperature dependence of the (a) *g*-factor, (b) line width, and (c) integral intesnity for polycrystalline **2** determined under anaerobic conditions.

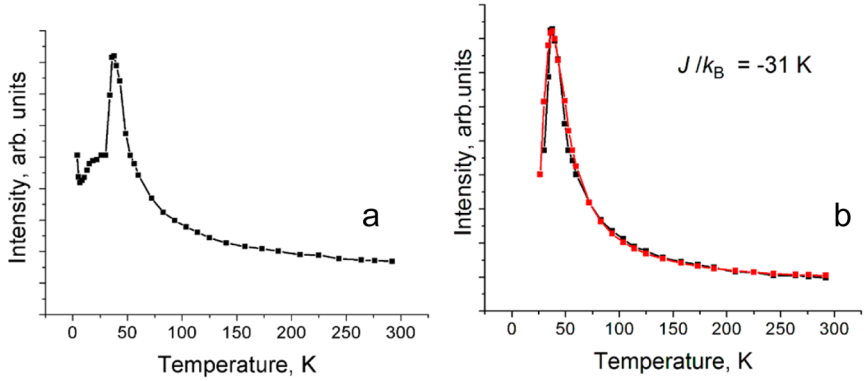

Figure 9. (a) Temperature dependence of total integral intensity of both narrow and broad EPR lines for polycrystalline sample of **2**; (b) fitting of the experimantal data (black) by the Heisenberg model for quadratic-layer antiferromagnetic coupling between spins[25] with exchange interaction $J/k_B = -31$ K (red).

Magnetic Properties. Compound **1** has no electron paramagnetic resonance (EPR) signal at room temperature due to the presence of the neutral tin(II) phthalocyanine and diamagnetic $Cp^*Ir^{III}I_2$ groups.

In accordance with its optical data, salt **2** contains the $C_{60}^{\bullet-}$ radical anions that manifest an intense EPR signal (Figure 7), whereas the $\{(Cp^*Ir^{III}I_2)Sn^{II}Pc(2-)$ units are EPR silent as in **1**. The EPR signal in **2** can be fitted by broad and narrow lines with g (g_1 and g_2) and line width (ΔH_{pp}) values of 1.9990 and 11.3 mT and 2.0007 and 0.493 mT, respectively, at room temperature (RT) (Figure 7). The parameters of the broad line allowed this signal to be attributed to $C_{60}^{\bullet-}$. The narrow lines were originally attributed to the disproportionation of $C_{60}^{\bullet-}$ to neutral and dianionic species[23a] or the Jahn–Teller effect in $C_{60}^{\bullet-}$ and thermal population of closely lying excited states.[14a,23b] Later, it was found that such narrow signals (ΔH = 0.1–0.2 mT) can appear due to the formation of $C_{120}O$[24a] or oxidation of $C_{60}^{\bullet-}$ by traces of oxygen.[24b,c] Notably, the broad signal becomes significantly narrower and shifts to larger *g*-factors as the temperature decreases to 38 K, while the narrow line exhibits a nearly temperature-independent *g*-factor and line width (Figure 8a and b, respectively). The integral intensity of the broad line reaches a maximum at 38 K, followed by an abrupt decrease below this temperature (Figure 8c), most likely due to antiferromagnetic ordering of the spins in the fullerene chains. In addition, the integral intensity of the narrow line is

DOI: 10.1021/om501210s
Organometallics 2015, 34, 879–889

only 2% that of the broad line. Furthermore, the intensities of the narrow and broad lines exhibit very similar temperature dependence behavior (Figure 8c). Therefore, the spins contributing to the narrow line are also involved in the antiferromagnetic ordering between the spins below 38 K (Figure 8c), and most likely the narrow line cannot be attributed to oxidation products of $C_{60}^{\bullet-}$ in **2**. The temperature dependence of the total integral intensity can be well reproduced using the Heisenberg model for quadratic-layer antiferromagnetic coupling between spins[25] with an exchange interaction J/k_B of −31 K, indicating strong antiferromagnetic coupling between the spins (Figure 9). Below 38 K, the *g*-factors of both the broad and narrow lines shift to smaller values (Figure 8a), and the width of the broad line is noticeably increased (Figure 8b). This behavior is also in agreement with low-temperature antiferromagnetic ordering of spins. Because the overlap integral between the $C_{60}^{\bullet-}$ molecules in each $C_{60}^{\bullet-}$ chain of **2** is moderate but uniform at 100 K (2.00×10^{-3} based on AM1 parametrization using the same method employed for the compound $(MDABCO^+)(C_{60}^{\bullet-})$TPC, where $MDABCO^+$ is *N*-methyldiazabicyclooctanium and TPC is triptycene),[1c] the antiferromagnetic coupling between $C_{60}^{\bullet-}$ radical anions in **2** can be also mediated by the $\pi-\pi$ interactions between the $C_{60}^{\bullet-}$ and Pc subsystems described in the Crystal Structures section (Figure 5a).

The compounds $(TBA^+)\{(Cp^*Ir^{II}X(\eta^2\text{-}C_{60}^-)\}$·solvent (**3** and **4**) are EPR silent at room temperature, and signals were also not detected at lower temperatures. Because the optical spectra described in the former section indicated the ionized state of C_{60} in these complexes, the electronic state is assigned as $(TBA^+)\{Cp^*Ir^{II}X(\eta^2\text{-}C_{60}^-)\}$, with two different components that each have the spin state $S = 1/2$. The very short distance between two spins (2−3 Å) and the formation of a coordination bond between these components should result in a diamagnetic state for the $\{Cp^*Ir^{II}X(\eta^2\text{-}C_{60}^-)\}$ anions. A small contribution of the $(TBA^+)\{(Cp^*)^-Ir^I(X^-)\}(\eta^2\text{-}C_{60})^0\}$ species is also possible, and in this case the Cp^*Ir^IX and C_{60}^0 units should also be diamagnetic and EPR silent. A similar diamagnetic state has also been observed for complexes of cobalt(II) tetraphenyl- or octaethylporphyrins with $C_{60}^{\bullet-}$ and $C_{60}(CN)_2^{\bullet-}$ radical anions.[26] Because the optical spectra of these complexes indicate that the fullerenes are negatively charged,[26e,f] both the porphyrins (Co^{II}TPP and Co^{II}OEP) and the fullerene radical anions ($C_{60}^{\bullet-}$ and $C_{60}(CN)_2^{\bullet-}$) should be paramagnetic with spin states of $S = 1/2$. However, the formation of Co(porphyrin)-C(fullerene$^-$) coordination bonds with lengths of 2.28−2.32 Å results in a diamagnetic EPR-silent state for the $\{Co^{II}TPP(C_{60})^-\}$, $\{Co^{II}TPP{\cdot}C_{60}(CN)_2^-\}$, and $\{Co^{II}OEP(C_{60})^-\}$ anions.[26]

CALCULATIONS

To examine the electronic structure of the $\{(Cp^*Ir^{II}I)(\eta^2\text{-}C_{60})\}$ units with C_1 symmetry, a theoretical analysis based on density functional theory (DFT) was performed[27] using the crystal structure data. The singlet and triplet states were investigated at the B3LYP and CAM-B3LYP/cc-pVTZ-PP/cc-pVDZ levels of theory. The results obtained using the B3LYP method were nearly the same as those obtained using CAM-B3LYP. The total and relative energies and $\langle S^2\rangle$ values are summarized in Table S3. Judging from the $\langle S^2\rangle$ values, spin contamination is nearly negligible for the calculated triplet states, because the $\langle S^2\rangle$ values for the pure triplet state are equal to 2. The B3LYP and CAM-B3LYP functionals indicate that the closed-shell singlet states are sufficiently energetically stable, and it is impossible to access the corresponding triplet states via thermal excitation. Therefore, the present DFT calculations support the diamagnetic nature of the $\{(Cp^*Ir^{II}I)(\eta^2\text{-}C_{60})^-\}$ anion observed using magnetic measurements. The energy diagram for the frontier Kohn−Sham orbitals in the singlet state is shown in Figure 10. The highest occupied molecular orbital

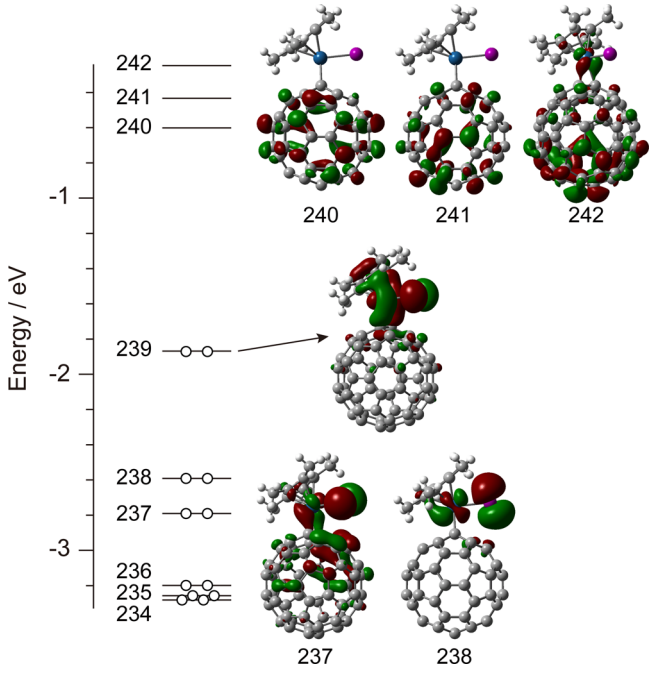

Figure 10. Energy diagram for the frontier Kohn−Sham orbitals of the ^1A state in the $\{(Cp^*Ir^{II}I)(\eta^2\text{-}C_{60}^-)\}$ anion calculated at the RB3LYP/cc-pVTZ-PP/cc-pVDZ level of theory. The 239th and 240th orbitals are the HOMO and LUMO, respectively.

(HOMO) is bonding among the iridium-d, Cp*-π, and C_{60}-π orbitals, and antibonding between the iridium-d and iodine-p orbitals. The lowest unoccupied molecular orbital (LUMO) and (LU+1)MO are localized on the C_{60} molecule. In addition, the bonding and antibonding orbital interactions of the central iridium-d orbital and Cp*-π, C_{60}-π, and iodine-p orbitals occur in the neighborhood of the frontier orbitals (Figure 10). To further evaluate the bond around the central iridium, Wiberg bond indices (WBIs)[28] were also estimated and are summarized in Table S4. The WBIs of the Ir−I, Ir−C_{60}, and Ir−Cp* bonds appear to be in the range of those for single, single, and double bonds, respectively, indicating the generation of diamagnetic species due to chemical bond formation. The calculated charge distributions are summarized in Table S5. Both Mulliken and natural population analyses indicate that the C_{60} molecule is negatively charged, and that the negative charges of the iodine and Cp* ring flow into the central iridium ion, which supports the anionic state of C_{60} observed in the NIR and IR spectra.

CONCLUSION

New synthetic methods were developed for the preparation of iridium coordination complexes with metal phthalocyanines and fullerene anions. The syntheses were performed using the radical anions of both the metal phthalocyanines and fullerenes. Using this method, the first crystalline coordination complex of a tin(II) phthalocyanine $\{(Cp^*Ir^{III}I_2)Sn^{II}Pc(2-)\}$ and the unusual salt **2** is constructed of closely packed chains from

DOI: 10.1021/om501210s
Organometallics 2015, 34, 879−889

$C_{60}^{\bullet-}$ and {(Cp*$Ir^{III}I_2$)Sn^{II}Pc(2−)}. The salt exhibits effective $\pi-\pi$ interactions between the fullerene and {(Cp*$Ir^{III}I_2$)Sn^{II}Pc(2−)} subsystems and strong magnetic coupling of the spins between the fullerenes. It should also be noted that the family of coordination complexes of metal phthalocyanines can be extended using compounds of different transition metals (Rh, Ru, Ir, and Mo), and this work is now in progress. Transition metal complexes with fullerene anions can also be obtained via the interaction of transition metals with the salts containing $C_{60}^{\bullet-}$ radical anions. The presence of donor Cp* ligands on a transition metal such as Ir^{II} does not allow the reduction of this metal by the C_{60}^{-} anions, and therefore the negative charge is localized on the fullerene molecule, as is observed in **3** and **4**. The formation of coordination complexes using two paramagnetic species (for example, Cp*M^{II}X and $C_{60}^{\bullet-}$) was also found to be accompanied by the formation of diamagnetic {(Cp*M^{II}X)(η^2-C_{60}^{-})} anions. Therefore, the preparation of similar transition metal complexes with diamagnetic metals should preserve the spins on the fullerene units, and such complexes may possess promising magnetic properties and high conductivity. Both methods allow the essential development of coordination chemistry using metal phthalocyanines and fullerenes and can provide novel functional compounds containing these interesting ligands.

EXPERIMENTAL SECTION

Materials. Tin(II) phthalocyanine (Sn^{II}Pc) was purchased from TCI, vanadyl phthalocyanine (V^{IV}OPc, 85%) was purchased from Acros, and TBABr (99%) was purchased from Aldrich. Fullerenes C_{60} (99.9%) and C_{70} (99%) were received from MTR Ltd. The (Cp*$Ir^{III}Cl_2$)$_2$ (>94%) and (Cp*$Ir^{III}I_2$)$_2$ dimers were purchased from TCI and Aldrich, respectively. Sodium fluorenone ketyl was obtained as described.[2d] Solvents were purified in an argon atmosphere. The *o*-dichlorobenzene ($C_6H_4Cl_2$) was distilled over CaH_2 under reduced pressure, and hexane was distilled over Na/benzophenone. Compounds **1**−**4** were synthesized and stored in an MBraun 150B-G glovebox with a controlled atmosphere containing less than 1 ppm each of water and oxygen. Solvents were degassed and stored in the glovebox, and the KBr pellets used for the IR and UV−visible−NIR analyses were prepared in the glovebox. EPR measurements were performed on polycrystalline samples of **1**−**4** sealed in 2 mm quarz tubes under 10^{-5} Torr.

Synthesis. Crystals of **1**−**4** were obtained using the diffusion technique. A reaction mixture in *o*-dichlorobenzene was filtered into a 1.8 cm diameter, 50 mL glass tube with a ground glass plug, and then 30 mL of hexane was layered over the solution. Slow mixing of the *o*-dichlorobenzene solution with hexane resulted in precipitation of crystals over 1−2 months. The solvent was then decanted from the crystals, and they were washed with hexane. The compositions of the obtained compounds were determined via X-ray diffraction analysis of a single crystal of each (see Supporting Information for X-ray diffraction data). Several different crystals were found to consist of one crystalline phase.

The compound {(Cp*$Ir^{III}I_2$)Sn^{II}Pc(2−)}·$2C_6H_4Cl_2$ (**1**) was obtained via the reduction of fullerene C_{70} (35 mg, 0.042 mmol) and tin(II) phthalocyanine (26.3 mg, 0.042 mmol) using a slight excess of sodium fluorenone ketyl (22 mg, 0.108 mmol) in 16 mL of *o*-dichlorobenzene in the presence of TBABr (30 mg, 0.092 mmol). The reaction was performed for 2 h at 100 °C. The resulting blue solution containing TBA^+ salts of $\{Sn^{II}Pc(3-)\}^{\bullet-}$ and $C_{70}^{\bullet-}$ was filtered into a flask containing the (Cp*$Ir^{III}I_2$)$_2$ dimer (25 mg, 0.022 mmol), and the solution was stirred for 1 day at 80 °C to produce a green solution. The solution was cooled to room temperature and filtered into a tube for diffusion. Large black prisms with a blue luster were obtained in 42% yield. The composition of **1** was confirmed via elemental analysis: Anal. Calcd for $C_{54}H_{39}Cl_4I_2IrN_8Sn$: C 41.19, H 2.67, N 7.68. Found: C 40.81, H 2.56, N 7.41.

The compound (TBA^+)($C_{60}^{\bullet-}$){(Cp*$Ir^{III}I_2$)Sn^{II}Pc(2−)}·$0.5C_6H_{14}$ (**2**) was obtained using a similar procedure to that described above for **1**, but 30 mg of C_{60} (0.042 mmol) was added to the reaction mixture instead of C_{70}. The addition of the (Cp*$Ir^{III}I_2$)$_2$ dimer (25 mg, 0.022 mmol) followed by stirring for 1 day at 80 °C produced a green solution, which was subsequently cooled to RT and filtered into a tube for diffusion. Black needles were obtained in 62% yield.

The compound (TBA^+){(Cp*Ir^{II}Cl)(η^2-C_{60}^{-})}·$1.34C_6H_4Cl_2$ (**3**) was obtained via the reduction of 30 mg (0.042 mmol) of C_{60} and 24.2 mg (0.042 mmol) of vanadyl phthalocyanine using a slight excess of sodium fluorenone ketyl (22 mg, 0.108 mmol) in 16 mL of *o*-dichlorobenzene in the presence of 2.2 equiv of TBABr (30 mg, 0.093 mmol). The reaction was performed for 2 h at 100 °C. The resulting blue solution containing TBA^+ salts of $\{V^{IV}OPc(3-)\}^{\bullet-}$ and $C_{60}^{\bullet-}$ was filtered into a flask containing the (Cp*$Ir^{III}Cl_2$)$_2$ dimer (17.4 mg, 0.022 mmol) and stirred at 80 °C for 6 h to afford a violet solution and V^{IV}OPc(2−) as a dark violet precipitate. The solution was then cooled to RT and filtered into a tube for diffusion. Black prisms of **3** were obtained in 42% yield.

The crystals of (TBA^+){(Cp*Ir^{II}I)(η^2-C_{60}^{-})}·$1.3C_6H_4Cl_2$·$0.2C_6H_{14}$ (**4**) were obtained similarly via the reduction of C_{60} and vanadyl phthalocyanine, but after the reduction the solution was filtered into a flask containing (Cp*$Ir^{III}I_2$)$_2$ (25 mg, 0.022 mmol). This solution was stirred at 80 °C for 6 h to afford a violet solution and a dark violet precipitate. The solution was subsequently cooled to room temperature and filtered to remove the V^{IV}OPc(2−). Black prisms of **4** were obtained in 67% yield.

Due to the extreme air sensitivity of **2**−**4**, their compositions were determined via X-ray diffraction analysis of single crystals of each compound. Elemental analysis could not be used to determine the compositions of **2**−**4** because they react with oxygen in the air before the quantitative oxidation procedure can be performed.

Computational Details. DFT calculations were performed using the unrestricted and restricted methods[29] based on B3LYP[29a] and CAM-B3LYP.[29b] The cc-pVTZ-PP basis set and the cc-pVDZ basis set were used for the Ir and I atoms[29c−f] and C and H atoms,[29g] respectively. Although the open-shell singlet states were calculated by generating the initial unrestricted wave functions, which were obtained using the HOMO−LUMO mixing or fragment guess methods for antiferromagnetic coupling, the results were the same as those obtained using restricted calculations. The stabilities of the wave functions were justified by specifying the "Stable=Opt" keyword in the present DFT calculations. The subsequent natural bond orbital (NBO) analysis was performed using the NBO program.[30] All computations were performed with the Gaussian 09 program package.[27]

ASSOCIATED CONTENT

Supporting Information

Starting materials, equipment used, crystallographic data, and IR spectra of **1**−**4**, structural view of **1**, and details of the DFT calculations for **4** are available free of charge via the Internet at http://pubs.acs.org.

AUTHOR INFORMATION

Corresponding Author

*E-mail (D. V. Konarev): konarev@icp.ac.ru. Fax: +7 49652-21852.

Notes

The authors declare no competing financial interest.

ACKNOWLEDGMENTS

The work was supported by Russian Science Foundation (project no. 14-13-00028) and a Grant-in-Aid for Scientific Research from JSPS, Japan (23225005 and 26288035). Y.N. is indebted to the JGC-S Scholarship Foundation. Theoretical

DOI: 10.1021/om501210s
Organometallics 2015, 34, 879−889

calculations were mainly performed at the Research Center for Computational Science, Okazaki, Japan.

REFERENCES

(1) (a) Guldi, D. M. *Chem. Soc. Rev.* **2002**, *31*, 22−36. (b) Tanigaki, K.; Prassides, K. *J. Mater. Chem.* **1995**, *5*, 1515−1527. (c) Konarev, D. V.; Khasanov, S. S.; Otsuka, A.; Maesato, M.; Saito, G.; Lyubovskaya, R. N. *Angew. Chem., Int. Ed. Engl.* **2010**, *49*, 4829−4832. (d) Gotschy, B. *Fullerene Sci. Technol.* **1996**, *4*, 677−698. (e) Nyokong, T. *Coord. Chem. Rev.* **2007**, *251*, 1707−1722. (f) Inabe, T.; Tajima, H. *Chem. Rev.* **2004**, *104*, 5503−5534. (g) Rittenberg, D. K.; Baars-Hibbe, L.; Böhm, A. B.; Miller, J. S. *J. Mater. Chem.* **2000**, *10*, 241−244.

(2) (a) Fagan, P. J.; Calabrese, J. C.; Malone, B. *Science* **1991**, *252*, 1160−1161. (b) Balch, A. L.; Catalano, V. J.; Lee, J. W.; Olmstead, M. M. *J. Am. Chem. Soc.* **1992**, *114*, 5455−5457. (c) Fagan, P. J.; Calabrese, J. C.; Malone, B. *Acc. Chem. Res.* **1992**, *25*, 134−142. (d) Konarev, D. V.; Khasanov, S. S.; Yudanova, E. I.; Lyubovskaya, R. N. *Eur. J. Inorg. Chem.* **2011**, 816−820. (e) Konarev, D. V.; Troyanov, S. I.; Khasanov, S. S.; Lyubovskaya, R. N. *J. Coord. Chem.* **2013**, *66*, 4178−4187. (f) Konarev, D. V.; Khasanov, S. S.; Troyanov, S. I.; Nakano, Y.; Ustimenko, K. A.; Otsuka, A.; Yamochi, H.; Saito, G.; Lyubovskaya, R. N. *Inorg. Chem.* **2013**, *52*, 13934−13940. (g) Balch, A. L.; Olmstead, M. M. *Chem. Rev.* **1998**, *98*, 2123−2165.

(3) (a) Balch, A. L.; Lee, J. W.; Noll, B. C.; Olmstead, M. M. *Inorg. Chem.* **1994**, *33*, 5238−5243. (b) Balch, A. L.; Hao, L.; Olmstead, M. M. *Angew. Chem., Int. Ed. Engl.* **1996**, *35*, 188−190. (c) Fagan, P. J.; Calabrese, J. C.; Malone, B. *J. Am. Chem. Soc.* **1991**, *113*, 9408−9409.

(4) (a) Lee, K.; Song, H.; Kim, B.; Park, J. T.; Park, S.; Choi, M.-G. *J. Am. Chem. Soc.* **2002**, *124*, 2872−2873. (b) Lee, G.; Cho, Y.-J.; Park, B. K.; Lee, K.; Park, J. T. *J. Am. Chem. Soc.* **2003**, *125*, 13920−13921. (c) Jin, X.; Xie, X.; Tang, K. *Chem. Commun.* **2002**, 750−751. (d) Konarev, D. V.; Troyanov, S. I.; Nakano, Y.; Otsuka, A.; Yamochi, H.; Saito, G.; Lyubovskaya, R. N. *Dalton Trans.* **2014**, *43*, 17920−17923. (e) Konarev, D. V.; Khasanov, S. S.; Nakano, Y.; Otsuka, A.; Yamochi, H.; Saito, G.; Lyubovskaya, R. N. *Inorg. Chem.* **2014**, *53*, 11960−11965. (f) Konarev, D. V.; Troyanov, S. I.; Nakano, Y.; Ustimenko, K. A.; Otsuka, A.; Yamochi, H.; Saito, G.; Lyubovskaya, R. N. *Organometallics* **2013**, *32*, 4038−4041.

(5) (a) Bengough, M. N.; Thompson, D. M.; Baird, M. C.; Enright, G. D. *Organometallics* **1999**, *18*, 2950−2952. (b) Thompson, D. M.; Bengough, M. N.; Baird, M. C. *Organometallics* **2002**, *21*, 4762−4770. (c) Thompson, D. M.; Brownie, J. H.; Baird, M. C. *Fullerenes, Nanotubes, Carbon Nanostruct.* **2004**, *12*, 697−713. (d) Thompson, D. M.; Jones, M.; Baird, M. C. *Eur. J. Inorg. Chem.* **2003**, 175−180. (e) Thompson, D. M.; McLeod, J.; Baird, M. C. *Pure Appl. Chem.* **2001**, *73*, 287−289.

(6) (a) Goldner, M.; Huckstadt, H.; Murray, K. S.; Moubaraki, B.; Homborg, H. *Z. Anorg. Allg. Chem.* **1998**, *624*, 288−294. (b) Barbe, J.-M.; Morata, G.; Espinosa, E.; Guilard, R. *J. Porphyrins Phthalcyanines* **2003**, *7*, 120−124. (c) Yang, C.-H.; Dzugan, S. J.; Goedken, V. L. *Chem. Commun.* **1986**, *24*, 1313−1315. (d) Guilard, R.; Kadish, K. M. *Comments Inorg. Chem.* **1988**, *7*, 287−305.

(7) Contakes, S. M.; Beatty, S. T.; Dailey, K. K.; Rauchfuss, T. B.; Fenske, D. *Organometallics* **2000**, *19*, 4767−4774.

(8) (a) Dailey, K. K.; Rauchfuss, T. B. *Angew. Chem., Int. Ed. Engl.* **1996**, *35*, 1833−1835. (b) Dailey, K. K.; Rauchfuss, T. B. *Polyhedron* **1997**, *16*, 3129−3136.

(9) (a) Onaka, S.; Kondo, Y.; Yamashita, M.; Tatematsu, Y.; Kato, Y.; Goto, M.; Ito, T. *Inorg. Chem.* **1985**, *24*, 1070−1076. (b) Zhong, X.; Feng, Y.; Ong, S.-L.; Hu, J.; Ng, W.-J.; Wang, Z. *Chem. Commun.* **2003**, 1882−1883. (c) Richard, P.; Zrineh, A.; Guilard, R.; Habbou, A.; Leconte, C. *Acta Crystallogr. Sect. C* **1989**, *45*, 1224−1226.

(10) Frampton, S. C.; Silver, J. *Inorg. Chem. Acta* **1986**, *112*, 203−204.

(11) (a) Balch, A. L.; Olmstead, M. M.; Oram, D. E.; Reedy, P. E., Jr.; Reimer, S. H. *J. Am. Chem. Soc.* **1989**, *111*, 4021−4028. (b) Adams, R. D.; Fang, F.; Smith, M. D.; Zhang, Q. *J. Organomet. Chem.* **2011**, *696*, 2904−2909.

(12) Konarev, D. V.; Kuzmin, A. V.; Faraonov, M. A.; Ishikawa, M.; Nakano, Y.; Khasanov, S. S.; Otsuka, A.; Yamochi, H.; Saito, G.; Lyubovskaya, R. N. *Chem.—Eur. J.* **2015**, *21*, 1014−1028.

(13) (a) Konarev, D. V.; Zorina, L. V.; Khasanov, S. S.; Litvinov, A. L.; Otsuka, A.; Yamochi, H.; Saito, G.; Lyubovskaya, R. N. *Dalton Trans.* **2013**, *42*, 6810−6816. (b) Konarev, D. V.; Kuzmin, A. V.; Khasanov, S. S.; Otsuka, A.; Yamochi, H.; Saito, G.; Lyubovskaya, R. N. *Dalton Trans.* **2014**, *43*, 13061−13069. (c) Konarev, D. V.; Kuzmin, A. V.; Simonov, S. V.; Khasanov, S. S.; Otsuka, A.; Yamochi, H.; Saito, G.; Lyubovskaya, R. N. *Dalton Trans.* **2012**, *41*, 13841−13847.

(14) (a) Reed, C. A.; Bolskar, R. D. *Chem. Rev.* **2000**, *100*, 1075−1120. (b) Konarev, D. V.; Lyubovskaya, R. N. *Russ. Chem. Rev.* **2012**, *81*, 336−366. (c) Semkin, N. V.; Spitsina, N. G.; Krol, S.; Graja, A. *Chem. Phys. Lett.* **1996**, *256*, 616−622.

(15) Picher, T.; Winkler, R.; Kuzmany, H. *Phys. Rev. B* **1994**, *49*, 15879−15889.

(16) Dubois, D.; Kadish, K. M.; Flanagan, S.; Haufler, R. E.; Chibante, L. P. F.; Wilson, L. J. *J. Am. Chem. Soc.* **1991**, *113*, 4364−4366.

(17) Robbins, J. L.; Edelstein, N.; Spencer, B.; Smart, J. C. *J. Am. Chem. Soc.* **1982**, *104*, 1882−1893.

(18) (a) Wan, W. C.; Liu, X.; Sweeney, G. M.; Broderick, W. E. *J. Am. Chem. Soc.* **1995**, *117*, 9580−9581. (b) Konarev, D. V.; Khasanov, S. S.; Otsuka, A.; Saito, G. *J. Am. Chem. Soc.* **2002**, *124*, 8520−8521. (c) Konarev, D. V.; Khasanov, S. S.; Saito, G.; Vorontsov, I. I.; Otsuka, A.; Lyubovskaya, R. N.; Antipin, Yu. M. *Inorg. Chem.* **2003**, *42*, 3706−3708. (d) Boyd, P. D. W.; Bhyrappa, P.; Paul, P.; Stinchcombe, J.; Bolkar, R. D.; Sun, Y.; Reed, C. A. *J. Am. Chem. Soc.* **1995**, *117*, 2907−2914.

(19) Kubiak, R.; Janczak, J. *J. Alloys Compd.* **1992**, *189*, 107−111.

(20) (a) Mavunkal, I. J.; Chi, Y.; Peng, S.-M.; Lee, G.-H. *Organometallics* **1995**, *14*, 4454−4456. (b) Burlakov, V. V.; Usatov, A. V.; Lysenko, K. A.; Antipin, M. Yu.; Novikov, Yu. N.; Shur, V. B. *Eur. J. Inorg. Chem.* **1999**, 1855−1857.

(21) Koefod, R. S.; Hudgens, M. F.; Shapley, J. R. *J. Am. Chem. Soc.* **1991**, *113*, 8957−8958.

(22) (a) Balch, A. L.; Catalano, V. J.; Lee, J. W. *Inorg. Chem.* **1991**, *30*, 3980−3981. (b) Balch, A. L.; Lee, J. W.; Noll, B. C.; Olmstead, M. M. *J. Am. Chem. Soc.* **1992**, *114*, 10984−10985. (c) Lee, J. W.; Olmstead, M. M.; Vickery, J. S.; Balch, A. L. *J. Cluster Sci.* **2000**, *11*, 67−77. (d) Usatov, A. V.; Martynova, E. V.; Dolgushin, F. M.; Peregudov, A. S.; Antipin, M. Y.; Novikov, Y. N. *Eur. J. Inorg. Chem.* **2002**, 2565−2567. (e) Balch, A. L.; Lee, J. W.; Noll, B. C.; Olmstead, M. M. *Inorg. Chem.* **1994**, *33*, 5238−5243.

(23) (a) Moriyama, H.; Kabayashi, H. *J. Am. Chem. Soc.* **1993**, *115*, 1185−1187. (b) Bhyrappa, P.; Paul, P.; Stinchcombe, J.; Boyd, P. D. W.; Reed, C. A. *J. Am. Chem. Soc.* **1993**, *115*, 11004−11005.

(24) (a) Paul, P.; Kim, K.-C.; Sun, D.; Boyd, P. D. W.; Reed, C. A. *J. Am. Chem. Soc.* **2002**, *124*, 4394−4401. (b) Litvinov, A. L.; Konarev, D. V.; Yudanova, E. I.; Kaplunov, M. G.; Lyubovskaya, R. N. *Russ. Chem. Bull.* **2002**, *51*, 2003−2007. (c) Konarev, D. V.; Kuzmin, A. V.; Khasanov, S. S.; Otsuka, A.; Yamochi, H.; Saito, G.; Lyubovskaya, R. N. *New J. Chem.* **2013**, *37*, 2521−2527.

(25) Lines, M. E. *J. Phys. Chem. Solids* **1970**, *31*, 101−l16.

(26) (a) Konarev, D. V.; Khasanov, S. S.; Otsuka, A.; Yoshida, Y.; Saito, G. *J. Am. Chem. Soc.* **2002**, *124*, 7648−7649. (b) Konarev, D. V.; Khasanov, S. S.; Otsuka, A.; Yoshida, Y.; Lyubovskaya, R. N.; Saito, G. *Chem.—Eur. J.* **2003**, *9*, 3837−3848. (c) Konarev, D. V.; Khasanov, S. S.; Otsuka, A.; Saito, G.; Lyubovskaya, R. N. *Chem.—Eur. J.* **2006**, *12*, 5225−5230. (d) Konarev, D. V.; Khasanov, S. S.; Otsuka, A.; Saito, G.; Lyubovskaya, R. N. *Dalton Trans.* **2009**, 6416−6420. (e) Konarev, D. V.; Khasanov, S. S.; Lyubovskaya, R. N. *Russ. Chem. Bull.* **2007**, *56*, 371−392. (f) Konarev, D. V.; Khasanov, S. S.; Lyubovskaya, R. N. *Coord. Chem. Rev.* **2014**, *262*, 16−36.

(27) Frisch, M. J.; Trucks, G. W.; Schlegel, H. B.; Scuseria, G. E.; Robb, M. A.; Cheeseman, J. R.; Scalmani, G.; Barone, V.; Mennucci, B.; Petersson, G. A.; Nakatsuji, H.; Caricato, M.; Li, X.; Hratchian, H. P.; Izmaylov, A. F.; Bloino, J.; Zheng, G.; Sonnenberg, J. L.; Hada, M.; Ehara, M.; Toyota, K.; Fukuda, R.; Hasegawa, J.; Ishida, M.; Nakajima,

DOI: 10.1021/om501210s
Organometallics 2015, 34, 879−889

T.; Honda, Y.; Kitao, O.; Nakai, H.; Vreven, T.; Montgomery, J. A., Jr.; Peralta, J. E.; Ogliaro, F.; Bearpark, M.; Heyd, J. J.; Brothers, E.; Kudin, K. N.; Staroverov, V. N.; Kobayashi, R.; Normand, J.; Raghavachari, K.; Rendell, A.; Burant, J. C.; Iyengar, S. S.; Tomasi, J.; Cossi, M.; Rega, N.; Millam, J. M.; Klene, M.; Knox, J. E.; Cross, J. B.; Bakken, V.; Adamo, C.; Jaramillo, J.; Gomperts, R.; Stratmann, R. E.; Yazyev, O.; Austin, A. J.; Cammi, R.; Pomelli, C.; Ochterski, J. W.; Martin, R. L.; Morokuma, K.; Zakrzewski, V. G.; Voth, G. A.; Salvador, P.; Dannenberg, J. J.; Dapprich, S.; Daniels, A. D.; Farkas, Ö.; Foresman, J. B.; Ortiz, J. V.; Cioslowski, J.; Fox, D. J. *Gaussian 09*, Revision D.01; Gaussian, Inc.: Wallingford, CT, 2009.

(28) Wiberg, K. B. *Tetrahedron* **1968**, *24*, 1083−1096.

(29) (a) Ragavachari, K. *Theor. Chem. Acc.* **2000**, *103*, 361−363 and references therein. (b) Yanai, T.; Tew, D.; Handy, N. *Chem. Phys. Lett.* **2004**, *393*, 51−57. (c) Peterson, K. A.; Shepler, B. C.; Figgen, D.; Stoll, H. *J. Phys. Chem. A* **2006**, *110*, 13877−13883. (d) Figgen, D.; Peterson, K. A.; Dolg, M.; Stoll, H. *J. Chem. Phys.* **2009**, *130*, 164108/1−11. (e) Feller, D. *J. Comput. Chem.* **1996**, *17*, 1571−1586. (f) Schuchardt, K. L.; Didier, B. T.; Elsethagen, T.; Sun, L.; Gurumoorthi, V.; Chase, J.; Li, J.; Windus, T. L. *J. Chem. Inf. Model.* **2007**, *47*, 1045−1052. (g) Dunning, T. H., Jr. *J. Chem. Phys.* **1989**, *90*, 1007−1023.

(30) Glendening, E. D.; Reed, A. E.; Carpenter, J. E.; Weinhold, F. *NBO* Version 3.1.

DOI: 10.1021/om501210s
Organometallics 2015, 34, 879−889